



Peak heights and peak widths at half-height in square wave voltammetry without and with ohmic potential drop for reversible and irreversible systems

Denise Krulic*, Nicolas Fatouros

Université Pierre et Marie Curie, Laboratoire PECSA-Electrochimie, 4, place Jussieu, 75252 Paris cedex 05, France

ARTICLE INFO

Article history:

Received 9 July 2010

Received in revised form 5 November 2010

Accepted 7 December 2010

Available online 15 December 2010

Keywords:

Square wave voltammetry

Peak current

Peak width at half-height

Ohmic potential drop

Uncompensated resistance

ABSTRACT

The behavior of voltammograms in square wave voltammetry in the presence of a significant ohmic potential drop for reversible and irreversible simple electrode reactions has been investigated. It is shown that the effects of ohmic potential drop can be drastically reduced by choosing adequately the square wave amplitude. Zone diagrams are drawn to define the conditions for which peak currents and peak widths at half-height can be expressed by simple formulas without considering the occurrence of ohmic potential drop. It follows that square wave voltammetry can be properly implemented in low-conductive media or in molten salt media where high concentrations of depolarizer are used.

© 2010 Elsevier B.V. All rights reserved.

1. Introduction

Theoretical results on the manifestations of ohmic potential drop in square wave voltammetry (SWV) have been published [1]. It has been concluded that, for a simple reversible reaction at the static mercury drop electrode (SMDE) with both redox forms soluble in an aqueous solution, the ohmic potential drop effects in SWV are negligible. Without fundamentally undermining this conclusion, we remark that when a mercury drop electrode is employed in a fully supported aqueous solution, the residual uncompensated resistance R_u can be five-fold higher than that taken into account in this report. For example, in 0.1 M KNO_3 R_u may reach 400 Ω [2–4]. Besides the uncompensated resistance of the solution, R_u includes external terms related to the electrical leads and to the working electrode. The measured resistance of SMDE EG&G PARC Model 303 electrodes is between 20 and 70 Ω [5] and that of carbon-modified electrodes, which constitute an effective alternative to the mercury electrode, is sometimes a few hundred ohms [6,7].

As we found ourselves with the Sn(II)/Sn(IV) couple in the LiCl-KCl eutectic at 450 °C [8], the problem of ohmic potential drop in SWV is real in molten salt media despite their high conductivity because of the large area of the electrodes and the high concentrations used. In these media, sometimes an additional resistance of a few ohms per square centimeter occurs due to the formation of poorly conducting oxide layers on electrodes during electrolysis [9]. The problem also arises with non-aqueous solutions of low

dielectric constant and high resistivity even after addition of quaternary ammonium salts [3,10,11].

In this work, a detailed description of SWV with consideration of the uncompensated resistance is achieved for reversible and totally irreversible electrode reactions. We found that the morphology of voltammograms depends greatly on the square wave amplitude especially for reversible systems. The fulfillment of certain conditions can virtually eliminate the effects of ohmic potential drop and facilitate the analysis of voltammograms.

In a first part, an assessment of the accuracy of approximate equations we have developed for the response in SWV without consideration of the ohmic potential drop is undertaken. The reference values were obtained from analytical solutions or by computer simulation performed with the required accuracy [12]. Emphasis is placed on the prediction of the half-height width of the voltammograms which provides a powerful intrinsic criterion of reversibility.

2. Notations in SWV

Let us use the following notations for the waveform in SWV shown in Fig. 1:

$$\begin{aligned}
 0 \leq t < t_1 & & E = E_1 \\
 t_{2j-1} < t < t_{2j} & & E = E_{2j} \\
 t_{2j} < t < t_{2j+1} & & E = E_{2j+1} \quad j > 0 \\
 t_{2j} - t_{2j-1} = t_{2j+1} - t_{2j} = \Delta t & & \\
 E_{2j} - E_{2j+1} = \Delta E & & \\
 E_{2j+1} - E_{2j-1} = \Delta E_s & &
 \end{aligned} \tag{1}$$

* Corresponding author. Tel.: +33 1 4427 2592.

E-mail address: denise.krulic@upmc.fr (D. Krulic).

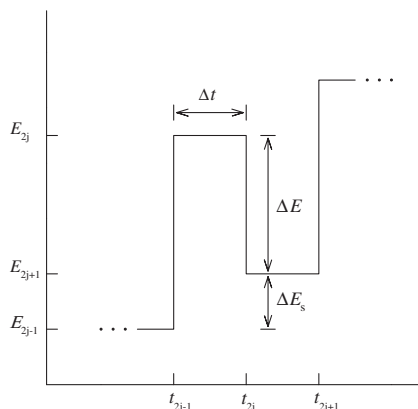


Fig. 1. Notations used for the waveform in SWV.

E is the potential applied to the electrode, $|\Delta E_s|$ the height of the step on the potential staircase and $|\Delta E|$ the height (edge to edge) of the pulse superimposed onto each step of the potential staircase. It is assumed that ΔE and ΔE_s have the same sign.

The current is sampled at $t_{2j} - 0$ and at $t_{2j+1} - 0$. The voltammogram, or peak, is obtained by interpolation of the discrete set of data points ($\Delta I = I(t_{2j}) - I(t_{2j+1})$, $E_{2j+1} + \Delta E/2$). In this work, peak currents ΔI_p and peak widths $w_{1/2}$ at half-height were determined from the theoretical data using respectively a sixth degree polynomial and a cubic Lagrange polynomial. In the ensuing development, each time reference is made to a function such as ΔI , it is implied that the interpolated curve is being referred to, whatever the method of interpolation used.

3. SWV without ohmic potential drop

We shall consider reversible and totally irreversible charge transfer reactions from one soluble state to another at a plane electrode and at the SMDE in the presence of an excess of indifferent electrolyte.

3.1. Dimensionless analysis

The use of dimensionless parameters and variables brings a universal character to the equations of voltammograms, transforming an individual situation described with dimensional numbers into a generic case. The dimensional analysis of the governing semi-infinite diffusion equations [12,13] leads to the dimensionless numbers listed in Table 1 where n is the number of electrons involved in the reaction, A the surface area of the electrode, c^* the bulk concentration of Ox or Red species initially present in solution, D its diffusion coefficient (i.e., D_{Ox} or D_{Red} as appropriate), r_0 the radius of the SMDE, E^0 the apparent standard potential of the

Table 1
Dimensionless numbers used in SWV for reversible and totally irreversible charge transfer reactions at a plane electrode and at the SMDE.

Reversible and irreversible reactions	
$\Delta\psi = \Delta I / nFAc^* \sqrt{D/\pi\Delta t}$	
$\gamma = \sqrt{D_{\text{Ox}}/D_{\text{Red}}}$	
$\delta = \sqrt{D\Delta t}/r_0$	
Reversible reaction	Irreversible reaction
$\mathcal{E} = nF(E_{2j+1} + \Delta E/2 - E^0)/RT$	$\mathcal{E}' = \alpha F(E_{2j+1} + \Delta E/2 - E^0)/RT$
$\Delta\mathcal{E}_s = nF\Delta E_s/RT$	$\Delta\mathcal{E}'_s = \alpha F\Delta E_s/RT$
$\Delta\mathcal{E} = nF\Delta E/RT$	$\Delta\mathcal{E}' = \alpha F\Delta E/RT$
$\omega_{1/2} = nFw_{1/2}/RT$	$\chi = k^0 \sqrt{\Delta t}/D$

redox couple, k^0 the standard rate constant and α the cathodic or anodic charge transfer coefficient. The other symbols have their usual meanings.

3.2. Simple formulas for the peak height and for the peak width at half-height

3.2.1. Reversible reaction

The result of using dimensionless numbers is a single equation for $\Delta\psi$ such as:

$$\Delta\psi = f(\mathcal{E}, \Delta\mathcal{E}_s, \Delta\mathcal{E}, \gamma, \delta) \quad (2)$$

For a plane electrode δ is zero. γ affects only the position of $\Delta\psi$ curve along the \mathcal{E} coordinate. Therefore, the dimensionless peak current $\Delta\psi_p$ and $\omega_{1/2}$ depend on $\Delta\mathcal{E}_s$ and $\Delta\mathcal{E}$, the pertinent parameter being $\Delta\mathcal{E}$.

For simplicity, in the examples to be presented, $n\Delta E_s$, $n\Delta E$ and $n\omega_{1/2}$ in mV at 25 °C will be considered. The corresponding non-dimensional values are obtained by dividing by $RT/F = 25.6926$ mV.

An analytical solution for $\Delta\psi$ involving partial sums exists in the case of a reversible electrode reaction with both redox forms soluble in solution at a plane electrode whatever γ and at the SMDE for $\gamma = 1$, i.e., when the diffusion coefficients of Ox and Red species can be considered equal [14–17]. In the other hand, there is no equation to our knowledge that can accurately predict the peak width.

The solution for $\Delta\psi$ can be split into two parts corresponding distinctly to $\Delta\mathcal{E}_s$ and $\Delta\mathcal{E}$, i.e., to the contributions of the potential staircase and of the pulses superimposed on the steps of this staircase [15,16]. After some algebra, the following simple approximation formula for $\Delta\psi_p$ is obtained [16,17]:

$$\Delta\psi_p = (1.2 + \Delta\mathcal{E}_s/2\Delta\mathcal{E})\tanh(\Delta\mathcal{E}/4)(1 + \sqrt{\pi}\delta/1.2) \quad (3)$$

$\Delta\psi_p$ has the sign of ΔE .

In Fig. 2, the percent error in the peak current introduced by the use of Eq. (3) for a plane electrode and for the SMDE are plotted against $n|\Delta E|/\text{mV}$ in the interval [10, 220] for three $n\Delta E_s/\text{mV}$ 2, 5, 10. The error is mostly less than 2%. In the case of the SMDE, calculations were carried out with $D = 10^{-5} \text{ cm}^2 \text{ s}^{-1}$, $\Delta t = 50 \text{ ms}$ and $r_0 = 0.0373 \text{ cm}$ which is the radius we measured for the medium

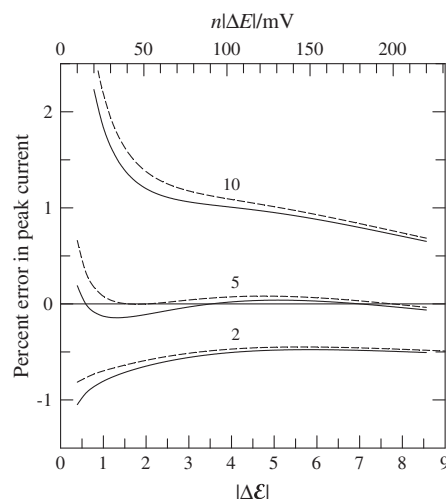


Fig. 2. Percent error in the peak current for a reversible reaction at a plane electrode (solid curves) and at the SMDE (dashed curves) introduced by Eq. (3) at 25 °C as a function of $n|\Delta E|/\text{mV}$ for various $n|\Delta E_s|/\text{mV}$ indicated near the curves. An axis for the corresponding dimensionless numbers $|\Delta\mathcal{E}| = nF|\Delta E|/RT$ is added to the graph. For the SMDE $\delta = \sqrt{D\Delta t}/r_0 = 0.019$. The exact values were calculated from equations given in Refs. [15,16].

drop of the PARC SMDE. For these values, δ is equal to 0.019. The contribution of the electrode curvature is in absolute 2.8%.

Let $\Delta\psi_1$ the main component of $\Delta\psi$ at a plane electrode which depends only on $\Delta\mathcal{E}$. $\Delta\psi_1$ can be accurately expressed as [16]:

$$\Delta\psi_1 = 1.2((1 + \gamma \exp(\mathcal{E}))^{-1} - (1 + \gamma \exp(\mathcal{E} + \Delta\mathcal{E}))^{-1}) \quad (4)$$

$\Delta\psi_1/1.2$ formally corresponds to the dimensionless current in differential pulse polarography (DPP) when the effect of the curvature of the SMDE is neglected.

The peak value of the bell-shaped curve $\Delta\psi_1 = f(\mathcal{E})$ is:

$$\Delta\psi_{p,1} = 1.2 \tanh(\Delta\mathcal{E}'/4) \quad (5)$$

The peak width ω_h of $\Delta\psi_1$, i.e., the dimensionless peak width in DPP, at any fraction h of its height, is obtained from Eqs. (4) and (5):

$$\omega_h = \frac{w_h nF}{RT} = \ln \left(\frac{b + \sqrt{b^2 - a}}{b - \sqrt{b^2 - a}} \right) \quad (6)$$

where

$$a = 4h^2 \exp(\Delta\mathcal{E}) \quad (7)$$

and

$$b = (1 - h)(1 + \exp(\Delta\mathcal{E})) + 2 \exp(\Delta\mathcal{E}/2) \quad (8)$$

Because of the contribution of the potential staircase, $w_{1/2}$ in SWV is a bit larger than in DPP especially for low $|\Delta\mathcal{E}|$. To take account of this enlargement, Eq. (6) can be used with h slightly below 0.5. For $n|\Delta\mathcal{E}_s|/\text{mV} \in [2, 10]$ and $n|\Delta\mathcal{E}|/\text{mV} \in [20, 220]$, $h = 0.464$ was fitted in order to minimize deviations between results obtained numerically and from Eq. (6). As it is shown in Fig. 3, the maximum absolute deviation is less than $0.5/n$ mV.

In the case of a reversible reaction at the SMDE with both redox forms soluble in solution, the influence of the curvature of the electrode on the peak width is not significant.

3.2.2. Irreversible reaction

For a unidirectional or “totally irreversible” electrochemical reaction $\Delta\psi$ is a function of dimensionless parameters, such that:

$$\Delta\psi = g(\mathcal{E}', \Delta\mathcal{E}'_s, \Delta\mathcal{E}', \chi, \gamma, \delta) \quad (9)$$

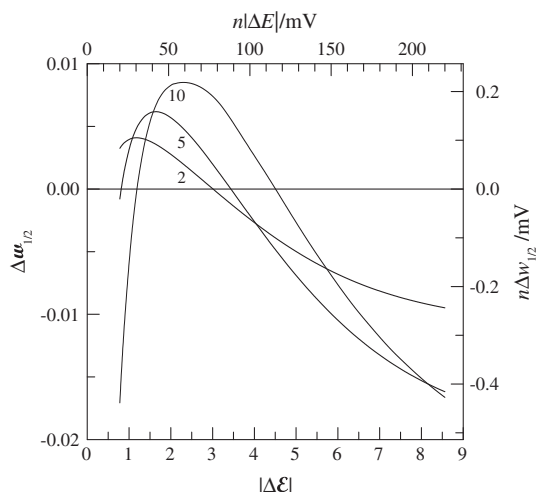


Fig. 3. Error in the peak width at half-height for a reversible reaction at a plane electrode, introduced by the use of Eq. (6) at 25 °C with $h = 0.464$. The deviation $n\Delta w_{1/2}/\text{mV}$ between values calculated numerically and from Eq. (6) is plotted as a function of $n|\Delta\mathcal{E}|/\text{mV}$ for various $n|\Delta\mathcal{E}_s|/\text{mV}$ indicated near the curves. Axes for the corresponding dimensionless numbers $\Delta w_{1/2} = nF\Delta w_{1/2}/RT$ and $|\Delta\mathcal{E}| = nF|\Delta\mathcal{E}|/RT$ are added to the graph.

The electrode reaction can be characterized as totally irreversible if $\chi < 3 \times 10^{-2}$. Changing χ in this domain does not affect the shape of $\Delta\psi$ curves. For a plane electrode $\Delta\psi_p$ depends only on $\Delta\mathcal{E}'$ and $\Delta\mathcal{E}'_s$.

When both redox forms are soluble in solution the peak current at a plane electrode and at the SMDE can be well approximated by the following equation [12,18]:

$$\Delta\psi_p = \pm 0.8 |\Delta\mathcal{E}'_s|^{0.405} \tanh(0.47 |\Delta\mathcal{E}'|) (1 + d) \quad (10)$$

where the minus sign applies for a reduction. The spherical correction d is given by:

$$d = 1.2 \delta |\Delta\mathcal{E}'_s|^{-0.5} (\Delta\mathcal{E}_s/\Delta\mathcal{E})^{-0.08} \quad (11)$$

The charge transfer coefficient α can be determined directly from the half-width $l_{1/2}$ at mid-height taken between the first side of the voltammogram in the direction of the scan and the vertical axis passing through its vertex. Actually, for $\alpha|\Delta\mathcal{E}_s| \leq 5$ mV and $\alpha|\Delta\mathcal{E}| < 60$ mV, $\alpha l_{1/2}/RT$ is equal to 1.70 ± 0.04 and then [12]:

$$\alpha = 1.7RT/l_{1/2}F \quad (12)$$

Fig. 4 shows that for $\alpha|\Delta\mathcal{E}_s|/\text{mV} \in [1, 5]$, $\alpha|\Delta\mathcal{E}|/\text{mV} \in [21, 90]$ and $\delta = 0.019$, the error introduced by Eq. (10) is always less than 2%. Note that the contribution of the electrode curvature on the peak current is considerably higher than that in the reversible case and lies between 5.7% ($\alpha|\Delta\mathcal{E}_s| = 5$ mV, $\alpha|\Delta\mathcal{E}| = 21$ mV) and 16.5% ($\alpha|\Delta\mathcal{E}_s| = 1$ mV, $\alpha|\Delta\mathcal{E}| = 90$ mV).

In summary, the error introduced by Eqs. (3), (6), and (10) for reversible and totally irreversible systems is within the margin of the experimental uncertainty. Actually, under favorable experimental conditions the uncertainty in the current measurement is less than $\pm 2.5\%$. The corresponding uncertainty on the peak width at half-height can be evaluated considering the difference between the widths taken at fractions of the peak height $h = (1 \pm 0.025)/2$ and at $h = 1/2$. Calculations show that this uncertainty is within $1.9/n$ and $2.5/n$ mV for $n|\Delta\mathcal{E}|/\text{mV} \in [20, 220]$ irrespectively of $\Delta\mathcal{E}_s$.

4. SWV with ohmic potential drop

In this section it will still be considered that the solution contains a supporting electrolyte in a sufficient excess to avoid signif-

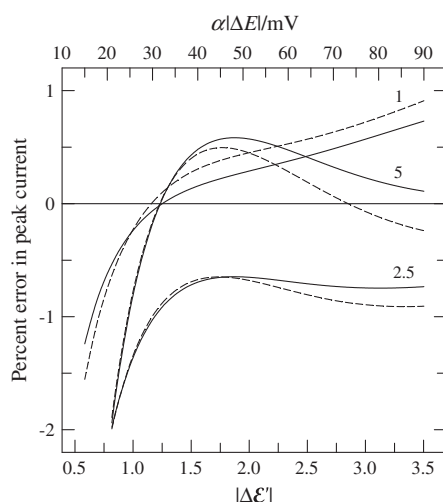


Fig. 4. Percent error in the peak current for a totally irreversible reaction at a plane electrode (solid curves) and at the SMDE (dashed curves) introduced by Eq. (10) at 25 °C as a function of $\alpha|\Delta\mathcal{E}|/\text{mV}$ for various $\alpha|\Delta\mathcal{E}_s|/\text{mV}$ indicated near the curves. An axis for the dimensionless number $|\Delta\mathcal{E}'| = \alpha F |\Delta\mathcal{E}|/RT$ is added to the graph. For the SMDE $\delta = \sqrt{D\Delta t}/r_0 = 0.019$. The reference values were calculated numerically.

icant contributions from the potential across the diffuse double layer, the change of the solution resistance, the change of activity and the migration in the electrical field of reducible or oxidable ions. For weakly supported solutions, an exact interpretation of voltammograms in SWV at various kinds of electrodes cannot be given at present. We note that, recently, studies have been presented concerning the effects of incomplete electrolytic support on cyclic voltammetry and chronoamperometry at macroelectrodes [19,20].

For a reversible reaction the occurrence of residual uncompensated resistance R_u is revealed by the dimensionless number:

$$\rho_u = n^2 F^2 A \sqrt{D} c^* R_u / \sqrt{\Delta t} RT \quad (13)$$

which arises from the ohmic potential drop expressed as: $\pm nFAD(\partial c/\partial x)_{x=0} R_u$. It is noted that in Ref. [1], where the square wave frequency is used instead of Δt , $\rho_u/\sqrt{2}$ was considered.

R_u can be determined by electrochemical impedance spectroscopy. In the case of the SMDE, the contribution of the solution resistance can be formally estimated from the conductivity of the solution [4]. For example, taking $100 \Omega^{-1} \text{cm}^2 \text{mol}^{-1}$ the molar conductivity at 25 °C of a 0.1 M uni-univalent supporting electrolyte, $n = 2$, $c^* = 10^{-3} \text{M}$, $D = 10^{-5} \text{cm}^2 \text{s}^{-1}$, $r_0 = 0.0373 \text{cm}$ and $\Delta t = 10 \text{ms}$, from Eq. (13) and Eq. (4) in Ref. [4] a significant value of ρ_u 2.5 is calculated. For an experiment in molten salt medium at 450 °C with $R_u = 1 \Omega$, $A = 1 \text{cm}^2$, $c^* = 10^{-2} \text{M}$ and with the same values for n , D and Δt , ρ_u is 2. However, note that for such experiments the concentration of the depolarizer is usually many times greater.

4.1. Reversible reaction

For a reversible reaction, $\Delta\psi_p$ and $\omega_{1/2}$ depend on ρ_u , $\Delta\mathcal{E}_s$, $\Delta\mathcal{E}$ and δ . In the case of a plane electrode the pertinent parameters are $\Delta\mathcal{E}$ and ρ_u .

The distortion of a voltage waveform around the peak of the voltammogram for $\rho_u = 2$ is shown in Fig. 5 where the actual potential at the working electrode and the applied potential are plotted together against time.

$|\Delta\psi_p|$ in Fig. 6 and $\omega_{1/2}$ in Fig. 7 are plotted as a function of ρ_u for $\delta = 0$, $n|\Delta\mathcal{E}_s| = 6 \text{mV}$ and for several values of $n|\Delta\mathcal{E}|/\text{mV}$.

The curves in Fig. 6 exhibit a maximum which grows and shifts towards higher ρ_u with increasing $n|\Delta\mathcal{E}|$. For ρ_u sufficiently large, $|\Delta\psi_p(\rho_u)|$ becomes smaller than $|\Delta\psi_p(0)|$. Therefore, on each curve there exists a point indicated by a triangle such that

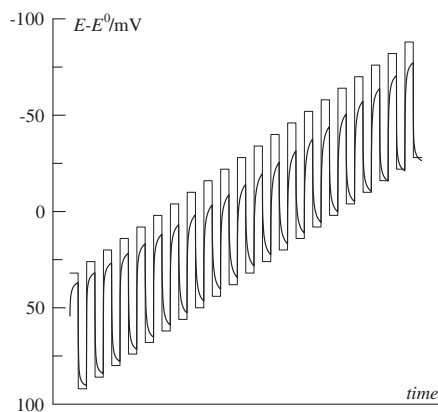


Fig. 5. Voltage actually applied to a plane electrode around the peak of the voltammogram for a reversible reaction (thick lines) and the rated voltage (thin lines). Conditions: Ox species initially present in solution, temperature 25 °C, $\rho_u = 2$, $n = 1$, $\Delta\mathcal{E}_s = -6 \text{mV}$ and $\Delta\mathcal{E} = -60 \text{mV}$. The dimensionless number ρ_u is defined by Eq. (13).

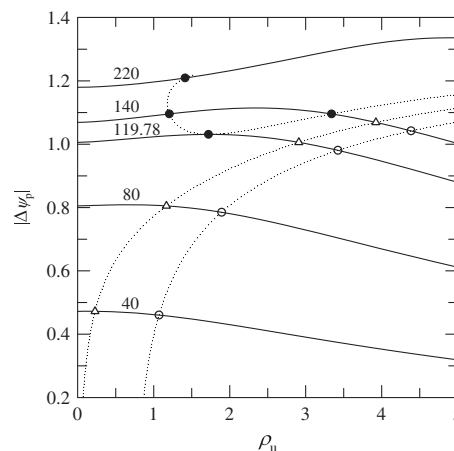


Fig. 6. Variation of the dimensionless peak current $|\Delta\psi_p|$ in the case of a reversible reaction at a plane electrode at 25 °C as a function of ρ_u for $n|\Delta\mathcal{E}_s| = 6 \text{mV}$ and several values of $n|\Delta\mathcal{E}|/\text{mV}$ indicated near the curves. For the points indicated by triangles the heights of peaks are the same as those for the peaks free of ohmic potential drop. For the points indicated by circles the relative deviation of heights is $\pm 2.5\%$ (hollow circles) or $\pm 2.5\%$ (filled circles).

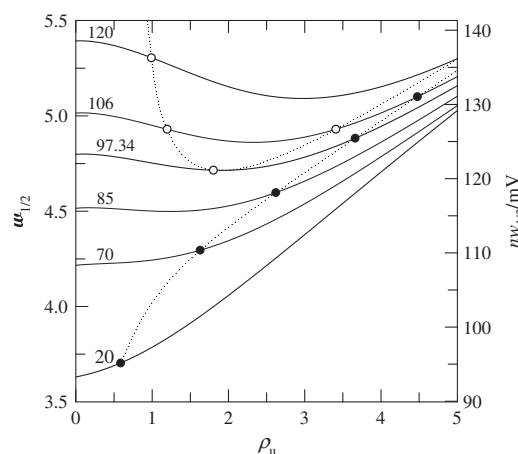


Fig. 7. Variation of the peak width at half-height $nw_{1/2}/\text{mV}$ in the case of a reversible reaction at a plane electrode at 25 °C as a function of ρ_u for $n|\Delta\mathcal{E}_s| = 6 \text{mV}$ and several values of $n|\Delta\mathcal{E}|/\text{mV}$ indicated near the curves. For the points indicated by filled and hollow circles $nw_{1/2}$ is equal to the widths of the free of ohmic potential drop peaks taken respectively at fractions 0.975/2 and 1.025/2 of their heights. An axis for the dimensionless width $\omega_{1/2} = nFw_{1/2}/RT$ is added to the graph.

$|\Delta\psi_p(\rho_u)| = |\Delta\psi_p(0)|$. Regarding the points indicated by circles, the relative deviation of $|\Delta\psi_p(\rho_u)|$ with respect to $|\Delta\psi_p(0)|$ is $\pm 2.5\%$. The points marked with filled circles correspond to the positive deviation. Such points exist only for $n|\Delta\mathcal{E}| \geq 119.78 \text{mV}$.

For points indicated by circles on curves in Fig. 7, the deviation of $\omega_{1/2}(\rho_u)$ with respect to $\omega_{1/2}(0)$ is equal to the uncertainty in $\omega_{1/2}(0)$ which arises from an uncertainty of $\pm 2.5\%$ on the half-height of the peak free of ohmic potential drop. The points marked with hollow circles correspond to the negative deviation. Such points exist only for $n|\Delta\mathcal{E}| \geq 97.34 \text{mV}$. In other words, for the filled circles $\omega_{1/2}(\rho_u)$ is equal to the dimensionless width $\omega_h(0)$ of the peak free of ohmic potential drop taken at the fraction h of its height 0.975/2 and for the hollow circles $\omega_{1/2}(\rho_u)$ is equal to the width $\omega_h(0)$ taken at the fraction 1.025/2.

4.1.1. Zone diagram

The behavior of $|\Delta\psi_p|$ and of $\omega_{1/2}$ as a function of $\Delta\mathcal{E}$ and ρ_u , allows us to draw the zone diagram presented in Fig. 8, where set of

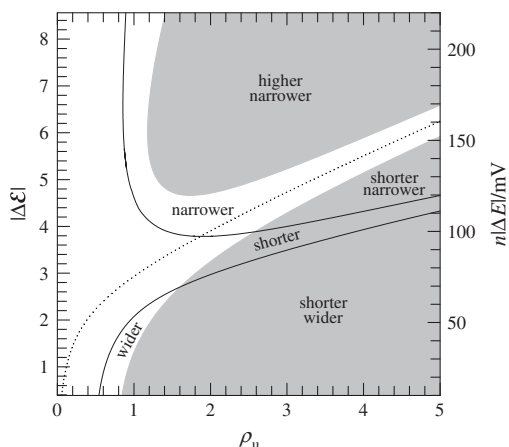


Fig. 8. Zone diagram for the behavior of peak currents and peak widths at half-height in the case of a reversible reaction at a plane electrode as a function of $n|\Delta E_s|/\text{mV}$ and ρ_u . For the construction of this diagram the deviations for the peak current and the peak width described in legends of Figs. 6 and 7 are taken into account.

points satisfying the certain given conditions for peak currents and peak half-height widths at a plane electrode, are plotted for $\rho_u \in [0, 5]$ and $n|\Delta E_s|/\text{mV} \in [10, 220]$ at 25 °C. $n|\Delta E_s|$ has been taken equal to 6 mV.

The edge of the lower shaded area is the set of points $(\rho_u, |\Delta\mathcal{E}|)$ where the relative deviation of the peak current with respect to the peak current free of ohmic potential drop is -2.5% . Similarly, on the edge of the upper shaded area the relative deviation of the peak current is $+2.5\%$. Therefore, in the unshaded area of the diagram the peak current is comparable within the experimental uncertainty to that obtained in the absence of ohmic potential drop.

On the dotted curve the peak current coincides with the peak current free of ohmic potential drop.

On the lower solid curve the half-height width of the peak is equal to the width of the free of ohmic potential drop peak taken at the fraction 0.975/2 of its height.

On the upper solid curve, the half-height width is equal to the width of the free of ohmic potential drop peak taken at the fraction 1.025/2 of its height.

The superimposition of the above solid curves on the areas relative to the peak height, delimits zones where the peak current is characterized as “higher” or “shorter” and the peak width at half-height as “narrower” or “wider” in comparison with the height and the width at half-height of the free of ohmic potential drop peak. The absence of one of these adjectives means that the quantity involved is virtually unchanged. What is unusual is that there is a zone where both peak height and half-height width decrease. However, the salient fact is that the use of $|\Delta E|$ between $100/n$ and $120/n$ mV overcomes the ohmic potential drop effects for ρ_u up to 2.6. Incidentally, in this range of $|\Delta E|$ the detection of residual uncompensated resistance by the deviation from linearity of the response as function of the square root of the frequency [1,21] becomes irrelevant.

Finally, it should be noted that this diagram is almost independent of $\Delta\mathcal{E}_s$.

The voltammograms presented in Fig. 9 illustrate the behavior that emerges from the zone diagram. They were calculated for a temperature of 25 °C, $n = 1$, $|\Delta E_s| = 6$ mV, $\rho_u = 3.92$ (thick curves) or $\rho_u = 0$ (thin curves) with 4 values of $|\Delta E|$ for which each point ($\rho_u = 3.9$, $|\Delta E|$) is located in a different zone of the diagram. Under the influence of the ohmic potential drop, the peaks become sharper. This is particularly visible at large $|\Delta E|$. For $|\Delta E| = 140$ mV the peaks calculated without and with ohmic potential drop have the same height.

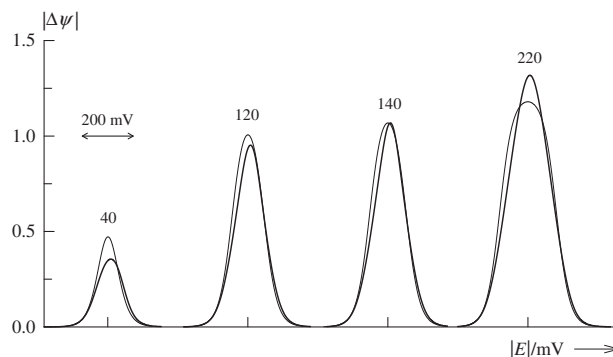


Fig. 9. Alteration of the shape of voltammograms in SWV resulting from a significant ohmic potential drop. Conditions: Temperature 25 °C, $n = 1$, $|\Delta E_s| = 6$ mV, $|\Delta E|/\text{mV}$ from left to right, 40, 120, 140, 220. ρ_u is taken 0 (thin curves) or 3.92 (thick curves). The vertical axis is common to all voltammograms. Ticks on the horizontal axis indicate for each curve the E^0 of the redox couple.

4.2. Irreversible reaction – Zone diagram

For a totally irreversible reaction the dimensionless parameter which takes into account the residual uncompensated resistance is:

$$\rho'_u = \alpha n F^2 A \sqrt{Dc} R_u / \sqrt{\Delta t} RT \quad (14)$$

Unlike the reversible case, $\Delta\psi_p$ and $w_{1/2}$ are strictly monotonic functions of ρ'_u . $|\Delta\psi_p|$ is decreasing and $w_{1/2}$ increasing.

The zone diagram presented in Fig. 10 is drawn for a plane electrode and three values of $\alpha|\Delta E_s|/\text{mV}$ 1, 2.5 and 5. For each value of $\alpha|\Delta E_s|$ the set of points $(\rho'_u, |\Delta\mathcal{E}'|)$ where the relative deviation of the peak current with respect to the peak current free of ohmic potential drop is -2.5% , is plotted for $\rho'_u \in [0, 2.5]$ and $\alpha|\Delta E|/\text{mV} \in [5, 110]$.

One can see that the influence of the ohmic potential drop on the peak current decreases with increasing $\alpha|\Delta E|$ and decreasing $\alpha|\Delta E_s|$. The use of low $|\Delta E_s|$ in order to counteract the effect of the ohmic potential drop should not be so determining for the signal to noise ratio. Indeed, for $\alpha|\Delta E| = 50$ mV, the change of $\alpha|\Delta E_s|$ from 5 to 1 mV leads to a decrease of $|\Delta\psi_p(0)|$ from 0.297 to 0.155 at 25 °C.

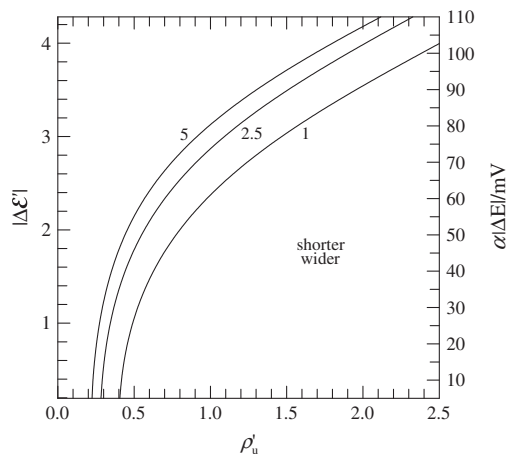


Fig. 10. Zone diagram for peak currents in the case of a totally irreversible reaction at a plane electrode for $\alpha|\Delta E_s|/\text{mV}$ 1, 2.5 and 5. For the construction of this diagram a deviation of -2.5% for the peak current with respect to that in the absence of ohmic potential drop is taken into account.

5. Conclusions

For a simple reversible electrode reaction, the response in SWV in the presence of a significant ohmic potential drop (high residual uncompensated resistance or high concentration of the depolarizer resulting in large currents) depends primarily on the magnitude of the pulse $|\Delta E|$ superimposed on each step of the potential staircase and on the dimensionless number ρ_u which is inversely proportional to the square root of the pulse duration Δt . ρ_u is calculated from Eq. (13) after evaluation of the residual uncompensated resistance.

The values of ρ_u and $n|\Delta E|$ show, through the zone diagram presented in Fig. 8, whether Eq. (3) for the peak current and Eq. (6), with $h = 0.464$, for the width at half-height of a free of ohmic potential drop voltammogram can be applied.

To minimize the effects of ohmic potential drop, large Δt , or low sampling frequencies, and $|\Delta E|$ around $120/n$ mV must be used. Such conditions make possible analytical determinations in low-conductive media, or direct determinations of high concentrations. In contrast, pulses of an amplitude $|\Delta E|$ less than $60/n$ mV can be used to reveal the occurrence of residual uncompensated resistance by the nonlinearity of the response as function of the square root of the frequency or by the peak-broadening.

For a totally irreversible simple reaction the response depends on ΔE , ΔE_s and the dimensionless number ρ'_u which includes the transfer coefficient α . ρ'_u is given by Eq. (14). The zone diagram presented in Fig. 10 shows whether Eq. (10) established for the peak current of a free of ohmic potential drop voltammogram can be ap-

plied. To minimize the effects of ohmic potential drop, Δt and $|\Delta E|$ must be increased and $|\Delta E_s|$ decreased.

References

- [1] V. Mirčeski, M. Lovrić, J. Electroanal. Chem. 497 (2001) 114–124.
- [2] J.B. Flanagan, K. Takahashi, F. Anson, J. Electroanal. Chem. 81 (1977) 261–273.
- [3] W.E. Thomas Jr, W.B. Schaap, Anal. Chem. 41 (1969) 136–142.
- [4] S.H. Hong, C. Kraiya, M.W. Lehmann, D.H. Evans, Anal. Chem. 72 (2000) 454–458.
- [5] Z. Kowalsky, K.H. Wong, R.A. Osteryoung, J. Osteryoung, Anal. Chem. 59 (1987) 2216–2218.
- [6] J. Navarro-Laboulais, J. Trijueque, J.J. Garcia-Jareno, F. Vicente, J. Electroanal. Chem. 422 (1997) 91–97.
- [7] C.M. Fioramonti Calixto, R.K. Mendes, A. Carlos de Oliveira, L.A. Ramos, P. Cervini, E.T. Gomes Cavalheiro, Mater. Res. 10 (2007) 109–114.
- [8] H. El Ghallali, H. Groult, A. Barhoun, K. Draoui, D. Krulic, F. Lantelme, Electrochim. Acta 54 (2009) 3152–3160.
- [9] A.E. Remick, H.W. McCormick, J. Electrochem. Soc. 102 (1955) 534–544.
- [10] K.M. Kadish, J.Q. Ding, T. Malinski, Anal. Chem. 56 (1984) 1741–1744.
- [11] J. Zhang, S.X. Guo, A. Bond, Anal. Chem. 79 (2007) 2276–2288.
- [12] N. Fatouros, D. Krulic, J. Electroanal. Chem. 443 (1998) 262–265.
- [13] J.C. Imbeaux, J.M. Savéant, J. Electroanal. Chem. 28 (1970) 325–338.
- [14] J.H. Christie, J.A. Turner, R.A. Osteryoung, Anal. Chem. 49 (1977) 1899–1903.
- [15] N. Fatouros, J.P. Simonin, J. Chevalet, J. Electroanal. Chem. 213 (1986) 1–16.
- [16] D. Krulic, N. Fatouros, M.M. El Belamachi, J. Electroanal. Chem. 385 (1995) 33–38.
- [17] N. Fatouros, D. Krulic, M. López-Tenés, M.M. El Belamachi, J. Electroanal. Chem. 405 (1996) 197–204.
- [18] D. Krulic, N. Fatouros, N. Larabi, E. Mahé, J. Electroanal. Chem. 601 (2007) 220–228.
- [19] E.J.F. Dickinson, J.G. Limon-Petersen, N.V. Rees, R.G. Compton, J. Phys. Chem. C 113 (2009) 11157–11171.
- [20] J.G. Limon-Petersen, J.T. Han, N.V. Rees, E.J.F. Dickinson, I. Streeter, R.G. Compton, J. Phys. Chem. C 114 (2010) 2227–2236.
- [21] A.V. Juarez, A.M. Baruzzi, L.M. Yudi, J. Electroanal. Chem. 577 (2005) 281–286.